Langmuir
Article
pubs.acs.org/Langmuir
© 2009 American Chemical Society

Comparative Study of Methane Adsorption on Single-Walled Carbon Nanotubes

Alberto G. Albesa, Edgardo A. Fertitta, and José L. Vicente*

Instituto de Investigaciones Fisicoquímicas Teóricas y Aplicadas (INIFTA), Departamento de Química, Facultad de Ciencias Exactas, UNLP, CC 16, Suc. 4 (1900) La Plata, Argentina

Received June 17, 2009. Revised Manuscript Received October 15, 2009

We present the combined results of ab initio and molecular mechanical calculations, computer simulations, and adsorption isotherms investigations of CH_4 adsorbed on HiPco single-walled carbon nanotubes. Isotherms and adsorption energies obtained in our model and simulations are in good agreement with ours and others experimental results. The theoretical analysis conducted for various homogeneous bundles of close-ended and open-ended tubes confirm not only the adsorption in at least two different stages but also the role played by each of the different adsorption sites on the nanotube bundles. The study of different site and nanotube sizes allows us to establish the presence of open tubes in the as-produced HiPco bundles, without regarding the role that adsorption in large interstitial channels may play. Our results also show that predicted scenarios, for the mechanism and the preferential adsorption sites depend on the size of the nanotubes and those of the bundles.

Introduction

The adsorption of methane at relatively low pressures on new carbonaceous materials developed from activated carbons, fullerenes, and nanotubes opens the possibility of interesting applications. One of them relates to the search and development of new storage systems for alternative fuels (natural gas, which consists mainly of methane, is one of the more promising options in this group).

Since their discovery, carbon nanotubes[1] have attracted a great deal of attention because of their novel structural and electronic properties.[2−5] The adsorption capacity of these materials is one of their more interesting properties related to gas storage.

A single-wall nanotube (SWNT) is formed from one graphene sheet rolled into a seamless cylinder of nanometric diameter and micrometric length. The nanotube's surface is closely related to that of graphite, which is considered as a standard substrate in studies of 2D adsorbed phases.[6] Moreover, nanotubes offer the opportunity to follow the dependence of the adsorbate's properties on the curvature of graphene planes and on confinement. (The latter raises the possibility of producing truly one-dimensional matter, either within the nanotubes themselves, or in the interstices between them, when they are grouped in bundles.)

Volumetric adsorption[7,8] is particularly well suited to study SWNTs, since their surfaces are uniform enough to adsorb simple molecules giving rise to stepwise isotherms. The adsorption isotherms measured on capped nanotubes generally exhibit two distinct bends, or substeps, which, while not vertical, are indicative of adsorption occurring on comparatively uniform fractions of the sample surface.

Methane adsorption isotherm on SWNTs provides evidence of these two types of distinct nonvertical substeps on the isotherms. The nonvertical nature of the substeps is the result of the presence of a distribution of adsorption energies and sizes in the adsorbing surfaces on the substrate.

There are different ways to produce nanotube bundles, for example, electric arc, laser ablation, and HiPco.[9,10] Nanotubes grown by the electric arc method tend to have capped ends,[11] while it has been suggested that as-produced HiPco nanotubes have a percentage of open nanotubes present.[12−16] It is therefore reasonable to think that nanotubes produced by different methods might exhibit somewhat different sorption properties. Recently some groups[17] have measured low coverage isosteric heats of adsorption (q_{st}) for Xe on nanotubes prepared from the arc and the HiPco methods, and found that q_{st} for Xe on the nanotubes produced by the electric arc method have considerably higher values than those for Xe on the HiPco nanotubes. By contrast, q_{st} values for Ar on electric arc nanotubes measured from other groups[18,19] at the same coverage are in good agreement. Hence, it

*To whom correspondence should be addressed. Tel.: 054-221-4257291. Fax: 054-221-4254642. E-mail: vicente@inifta.unlp.edu.ar.

(1) Iijima, S. *Nature* (*London*) **1991**, *354*, 56.
(2) Saito, R.; Dresselhaus, G.; Dresselhaus, M. S. *Physical Properties of Carbon Nanotubes*; Imperial College Press: London, 1998.
(3) Reich, S.; Thomsen, C.; Maultzsch, J. *Carbon Nanotubes: Basic Concepts and Physical Properites*; Willey−VCH: Weinheim, Germany, 2004.
(4) Migone, A. D.; Talapatra, S. In *Encyclopedia of Nanoscience and Nanotechnology*; Nalwa, H. S., Ed.; American Scientific: Los Angeles, CA, 2004.
(5) *Carbon Nanotubes: Science and Applications*; Meyyappan, M., Ed.; CRC: Moffett Field, CA, 2005.
(6) Albesa, A. G.; Llanos, J. L.; Vicente, J. L. *Langmuir* **2008**, *24*, 3836.
(7) Talapatra, S.; Migone, A. D. *Phys. Rev. B* **2002**, *65*, 045416.
(8) Muris, M.; Dufau, N.; Bienfait, M.; Dupont-Pavlovsky, N.; Grillet, Y.; Palmari, J. P. *Langmuir* **2000**, *16*, 7019.
(9) Dresselhaus, M. S.; Dresselhaus, G.; Avouris, P., Eds. *Carbon Nanotubes Synthesis, Structure, Properties, and Applications*; Springer-Verlag: Berlin, 2001.
(10) Bronikowski, M. J.; Willis, P. A.; Colbert, D. T.; Smith, K. A.; Smalley, R. E. *J. Vac. Sci. Technol. A* **2001**, *19*, 1800.
(11) Journet, C.; Bernier, P. *Appl. Phys. A: Mater. Sci. Process* **1998**, *67*, 1.
(12) Agnihotri, S.; Mota, J. P. B.; Rostam-Abadi, M.; Rood, M. J. *Langmuir* **2005**, *21*, 896.
(13) Du, W. F.; Wilson, L.; Ripmeester, J.; Dutrisac, R.; Simard, B.; Deommee, S. *Nano Lett.* **2002**, *2*, 343.
(14) Matranga, C.; Bockrath, B. J. *Phys. Chem. B.* **2004**, *108*, 6170.
(15) Kim, S.; Chen, L.; Johnson, J. K.; Marand, E. *J. Membr. Sci.* **2007**, *294*, 147.
(16) Agnihotri, S.; Zheng, Y.; Mota, J. P. B.; Ivanov, I.; Kim, P. *J. Phys. Chem. C* **2007**, *111*, 13747.
(17) Experimental results cited in: La Brosse, M.; Shi, W.; Johnson, J. K. *Langmuir* **2008**, *24*, 9430.
(18) Talapatra, S.; Rawat, D. S.; Migone, A. D. *Nanosci. Nanotechnol.* **2002**, *2*, 467.
(19) Wilson, T.; Tyburski, A.; DePies, M. R.; Vilches, O. E.; Becquet, D.; Bienfait, M. J. *Low Temp. Phys.* **2002**, *126*, 403.

appears that variations in sorption properties measured on nanotubes prepared by the same method (e.g., electric arc) are small compared with variations in those properties prepared by different methods. This implies that when comparing simulations and experiments, different atomic-scale models may be needed to accurately describe nanotube bundles produced through the electric arc and HiPco processes.

Theoretically, the first problem that has to be solved, when undertaking adsorption studies on nanotubes, is the identification of the adsorption sites. For SWNTs closed at both ends and aggregated into bundles, the possible adsorption sites are the interstitial channels (ICs), the convex external walls, or outer surface sites on the periphery of the bundles (S), and, the grooves between two adjacent outer nanotubes of the bundles (G).

Stan and Cole[20] presented one of the pioneering papers on the adsorption of rare gases in cylindrical pores that mimic nanotubes. They studied the low coverage adsorption and found great sensitivity to the species, the assumed potential model, and the radius of the tubes. In the limit of low coverage they adopted a potential inside the tube that smeared out the carbon atoms and omitted the atomistic details as well as the interaction between the adatoms. Analyzing the adsorption of CH_4 on graphite, we have shown[6] the relevance of the substrate structure when the coverage begins to grow, consequently the adequacy of the atom-smearing assumption should be reexamined.

Shi and Johnson computed isotherms and isosteric heats for Ar, CH_4, and Xe, using two different models of bundles: the "homogeneous" model consisting of identical diameter nanotubes packed on a hexagonal lattice; the "heterogeneous" model on the other hand, consider nanotubes with various diameters that were imperfectly packed, therefore, large interstitial defect sites are present. Many of these interstitial defect sites were large enough to allow adsorption of various gases. By contrast, the interstitial sites in the homogeneous bundle model did not accommodate adsorption of any of the gases they simulated. They found that, in contrast with the first model, the second one gave results consistent with experimental isosteric heat data[7,18,19,21] for electric arc nanotube samples.

Recent experiments and computer simulations results suggest that as-produced HiPco nanotubes are best modeled because they contain an open fraction of nanotubes.[12,13,15,16] From the experiments, it is not clear if models need to account for adsorption in interstitial channels in order to accurately describe the experimental data for HiPco SWNTs.

Up to now, the most common scenario proposed[22,23] to describe the adsorption process is as follows: it starts as linear chains at the strongest binding energy sites: grooves on the outside surface of the bundles and some larger, accessible, defect-induced interstitial channels. After these sites are filled, adsorption proceeds on the external surface of the bundles. The 2D adsorbate structure on the external bundle surface initially builds up adjacent to the occupied grooves until the entire external surface is covered by a single monolayer. The binding energies for this latter stage of adsorption are comparable but somewhat smaller than for adsorption on the basal plane of graphite, whereas the binding energy on the preferential adsorption sites (G, IC) populated during the initial stage of adsorption is considerably larger than that on planar graphite.

This explanation for simple gas adsorption on SWNT opens new challenging questions to be answered, for example: during the first stages of the process, between the more attractive sites like groove (G) and interstitial channels (ICs), which one begins to fill up first?, or in the case of opened tubes, what happens with the inner sites (T)? Of course the answers to these questions will depend on the kind of gas adsorbed and on the size of the nanotubes and bundles. Nevertheless, from the theoretical point of view Monte Carlo simulations add a new uncertainty because one needs to assume some potential model. The descriptions have to be based not only on statistical results derived from a potential imposed ad hoc, but also on ab initio and molecular mechanical calculations that give a self-consistent picture of the phenomenon.

The aim of this paper is to show the contribution of each group of adsorbing sites on the sorption process. We are not interested in comparing simulations utilizing complex models of nanotube bundles; instead, we mimic each adsorption zone with basic nanotubes bundles, in order to distinguish their contribution on the experimental data separately. In other words, we consider that simple models of nanotubes are capable of capturing the contribution of each group of adsorbing sites and that these models allow us to analyze them, in order to distinguish later their effect in the whole complex system, and to differentiate the nanotube samples produced by different synthesis techniques. With this goal, instead of adopting complex models, that in some cases might mask basic phenomena because of the superposition of a number of different causes, we adopted a model that is as simple as possible, while preserving the fundamental characteristics of the four basic sites of adsorption identified in the literature. We choose the smallest number of nanotubes that preserve these sites and consider nanotube diameters from 9.5 to 20.4 A approximately. Experimental nanotube bundles have, of course, a larger number of nanotubes, but from the point of view of the adsorption energy the values found from these bundles will be almost the same. For instance, interstitial defects derived from heterogeneous models can be mimicked by employing larger nanotubes of equal diameter, etc. On the other hand, if the contribution of each kind of site present in the bundle is known, one can later add their effect by multiplying by the corresponding number of this type of site in the bundle, and this can be done with arbitrary weight distributions. This approach would give the possibility of exploring many configurations with the sole constraint that results will be mean values, while heterogeneous models are limited to very few configurations observed experimentally. As a first step to follow these ideas we model the opened and closed nanotubes behavior.

Experimental Section

Adsorption isotherms at 77.7, 93, 103.2, 113, and 123.2 K, were volumetrically determined employing Pyrex conventional equipment. The isotherms measured at 77.7K, 103.2, and 113.2 K are shown in Figures 1, 2, and 3, respectively.

Pressures were determined using absolute capacitance manometers, MKS−Baratron 122 AA-00010AB, with 1.0×10^{-3} Torr maximum error. The temperatures were thermostatically controlled. Temperature was measured with a digital thermometer, Altronix, with a Pt-100 (DIN) sensor head previously calibrated against an oxygen vapor pressure thermometer with 0.1 K precision.[24] The gas that we used was from Matheson Gas Products. It had higher than 99% purity and was used in as received form, without any further purification. The sample of HiPco SWNTs, was from batch no. CAS 7782-42-5 (graphite),

(20) Stan, G.; Cole, M. W. *Surf. Sci.* **1998**, *395*, 280.
(21) Weber, S. E.; Talapatra, S.; Journet, C.; Zambano, A. Z.; Migone, A. D. *Phys. Rev. B* **2000**, *61*, 13150.
(22) Kuznetsova, A.; Yates, J., Jr.; Liu, J.; Smalley, R. E. *J. Chem. Phys.* **2001**, *114*, 4180.
(23) Bienfait, M.; Zeppenfield, P.; Dupont-Pavlovsky, N.; Muris, M.; Johnson, M. R.; Wilson, T.; DePies, M.; Vilches, O. E. *Phys. Rev. B* **2004**, *70*, 035410.
(24) Heroux, L.; Krungleviciute, V.; Calbi, M. M.; Migone, A. D. *J. Phys. Chem. B* **2006**, *110*, 12597.

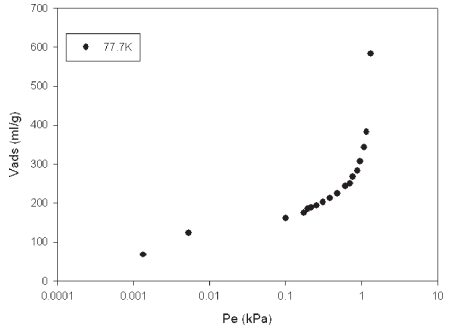

Figure 1. CH_4 adsorption isotherm at 77.7 K.

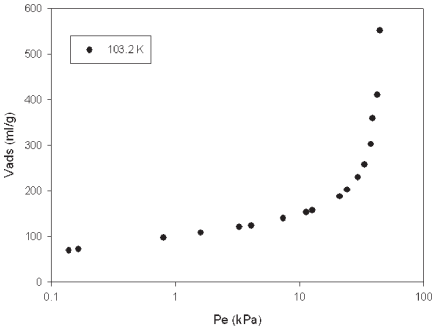

Figure 2. CH_4 adsorption isotherm at 103.2 K.

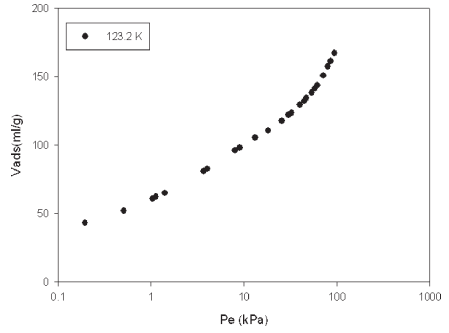

Figure 3. CH_4 adsorption isotherm at 123.2 K.

OSHA/PEL: 15 mg /m^3 (total dust), ACGIH/TLV: 2 mg /m^3 TWA, was produced by Unidym, Inc. (USA).

Experimentally it is possible to calculate the isosteric heat of adsorption Q_{st} of the gas adsorbed on the nanotubes from two isotherms determined at close but different temperatures, T_1 and T_2, via the equation

$$Q_{st} = \frac{RT^2}{(T_2 - T_1)} \ln\left(\frac{p_2}{p_1}\right) \quad (1)$$

where p_1 and p_2 are the equilibrium pressures at temperatures T_1 and T_2, respectively, when the amount of gas adsorbed is constant, and T is the corresponding mean temperature.

Ab Initio and Molecular Mechanical Calculations. In our simulations, the methane molecules can adsorb on the carbon nanotubes in four different types of sites: the grooves that are formed between two nanotubes (G sites), on the surface of the nanotube (S site), in interstitial channels (IC sites), and finally, in the case of opened nanotubes, inside the tubes (T sites).

The search for the less energetic sites was performed using the molecular dynamics module that is in the software package Hyperchem.[25] The force field of molecular mechanics MM+ available in this package was used for the simulations.

(25) *Hyper Chem. Release 7.0 for Windows, Molecular Modeling System; HyperCube*: http://www.hyper.com, **2002**.

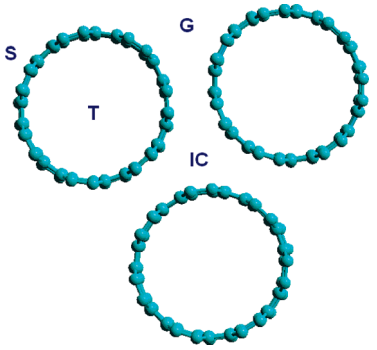

Figure 4. Simulation clusters, showing four types of adsorption sites: the grooves between two tubes (G sites); on the surface of the nanotube (S site); in the interior of the same (T sites), in the case of opened tubes; and in interstitial channels (IC sites).

To calculate the binding energy on each adsorption site, we employed a triangular array with three identical tubes as is shown in Figure 4.

Theoretical studies of gas adsorption have used many different nanotube diameters.[26] Here we consider three different nanotube diameters: 9.49, 16.28, and 20.34 A, corresponding to (7,7), (12,12), and (15,15) nanotubes in the armchair structure, respectively. The distance between the tubes or van der Waals gap was always 3.4 A. Some of these diameters are likely to be beyond the experimentally observed values,[23,27,28] but we consider that this range of diameters has a relevant role for CH_4 adsorption, taking into account that we will not describe some particular nanotube bundle. Instead of doing this, our aim is to identify the contribution of each group of adsorption sites in the adsorption process. Having adopted this point of view, we need not only know what happens in the IC, G, and C sites of homogeneous bundles, but also in the defect induced ICs of heterogeneous bundles. In our treatment we mimic the later by employing a simple homogeneous bundle but with nanotubes of bigger diameters, so that the ICs in this model are accessible for adsorption by methane (as are the defect-induced ICs of the heterogeneous bundles). This approach considers in a certain way the contribution of each site individually, or more precisely, groups the various independent regions, that is, external region of the bundles or G and C sites, internal regions of the bundles or IC sites, and internal tubes or T sites (in case of open nanotubes). For instance, we employ (7,7) and (12,12) nanotubes to mimic G, S, and T sites and (15,15) for IC sites. The limitations of this description are not so crude as to consider at low coverage, for instance, that adsorption takes place in IC and S sites at the same time; rather we take into account that when one begins the other can be almost complete, but detailed analysis of this point will require a detailed kinetic analysis that is beyond the scope of this work.[29]

The initial geometries were heated from 0 to 900 K in 0.1 ps, keeping the geometries of the nanotubes fixed. Then the temperature was maintained constant while docking the system to a thermal bath with a relaxation time of 0.05 ps. After balancing the system for 5 ps, 500 ps long simulations were carried out, during which the coordinates were saved every 1 ps. The optimized geometries were saved by using the force field MM+.

The calculations were made employing ab initio density functional theory (DFT), and using functional PW91PW91 and the set

(26) Shi, W.; Johnson, K. *Phys. Rev. Lett.* **2003**, *91*, 015504.
(27) Stan, G.; Bojan, M. J.; Curtarolo, S.; Gatica, S. M.; Cole, M. W. *Phys. Rev. B* **2000**, *62*, 2173.
(28) Cao, D.; Zhang, X.; Chen, J.; Wang, W.; Yun, J. *J. Phys. Chem. B* **2003**, *107*, 13286.
(29) Rawat, D. S.; Calbi, M. M.; Migone, A. D. *J. Phys. Chem. C* **2007**, *111*, 12980.

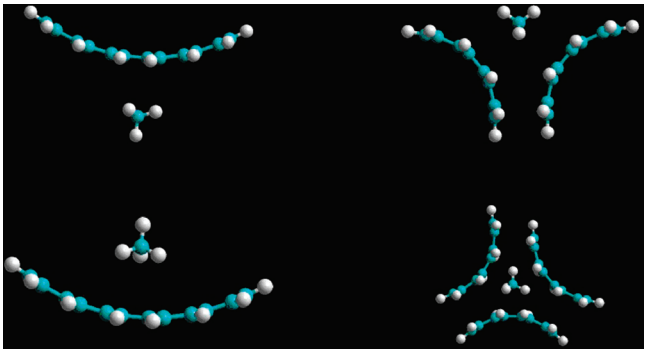

Figure 5. Optimized geometry, resulting from MM+ and DFT methods, for the four adsorption sites given in Figure 4: top left, top right, bottom left, (15,15); bottom right, (12,12).

of basis 6-31G (d, p). This functional was chosen because of its good behavior when studying systems with weak interactions.[28,30,31] To study these systems we used smaller clusters than those studied by the MM+ method. To achieve the minimum cluster size and to decrease the computational time, carbon atoms were removed from the nanotubes until the difference in interaction energy calculated between the methane molecule and the cluster was 10% of the energy calculated using the nanotubes. These clusters are shown in Figure 5.

The energy of interaction in both cases was calculated as

$$\Delta E(\text{int}) = E(\text{bundle} + \text{methane}) - E(\text{methane}) - E(\text{bundle}) \quad (2)$$

Grand Canonical Monte Carlo Ensemble. *Adsorbate−Adsorbate Interaction Potential*. We adopted the Martin and Siepmann model[32] to calculate the adsorbate−adsorbate interactions, because of its demonstrated capacity for reproducing experimental data over a wide range of pressures and temperatures.[33] Instead of changing the potentials, in order to match experimental values at some coverage region, we adopted graphite parameters for the nanotubes and clusters, because we have previously verified[34] that the dependence of these interaction parameters on curvature is negligible.

The interaction between methane molecules was modeled via a Lennard-Jones (L-J) 12−6 potential:

$$\varphi^{ff}(r) = 4\varepsilon^{ff}[(\sigma^{ff}/r)^{12} - (\sigma^{ff}/r)^{6}] \quad (3)$$

that describes the potential energy between two methane molecules at a distance r. The parameters employed in our calculations are given in Table 1.

Gas−Solid Potential. Simulations were performed using bundles of three nanotubes. The geometry of the bundles was optimized by employing the MM+ method.

The L-J interaction energy between methane molecules and nanotubes was considered to be pairwise additive: the interaction of a molecule with a cluster results from adding all L-J interactions with each C atom that constitutes each nanotube. The difference between this method and the commonly used continuous approximation was pointed by Albesa et al.[6] elsewhere.

Technical Simulation Details. The parameters used in the calculations associated with the simulations were (1) simulation box with a side length of 10 σ^{ff}; (2) the cut off radius was set to 2.5 σ^{ff}; (3) each simulation run consisted of 5×10^7 Monte Carlo steps that included the possibility of a creation, destruction, or displacement attempt for each molecule; 5×10^4 steps were taken for statistical averages; (4) periodic conditions were used in the z direction.

Another advantage of MC methods is that it is possible to obtain information on the isosteric heat of adsorption. The isosteric heat of adsorption $-\Delta H^0$ is the difference between the molar enthalpy of the sorbate in the vapor phase and the partial molar enthalpy of the adsorbed phase.

Table 1. Lennard-Jones Interaction Parameters[7]

	ε^{XX}/k_B	σ^{XX}/Å
methane (X = f)	148 K	3.81
graphite (X = s)	28 K	3.40

Table 2. Interaction Energies from MM+ Method

MM+ [KJ]	S	G	T	IC
7,7	−11.62	−23.28	−31.94	183.29
12,12	−13.23	−24.93	−21.21	−5.60
15,15	−13.77	−26.13	−19.14	−36.14

Table 3. Interaction Energies from DFT Method

DFT [KJ]	S	G	T	IC
7,7	−10.78	−20.34	−25.58	776.89
12,12	−13.33	−22.25	−17.42	142.29
15,15	−13.12	−15.11	−15.48	−18.54

Results and Discussions

Isotherms and Isosteric Heat of Adsorption Obtained from Experimental Results. In Figure 1 we display the adsorption isotherm measured at 77.3 K. By comparison, the adsorption isotherm of methane on graphite at this temperature has a single step in the monolayer regime at approximately 0.2 kPa. We note that one of the substeps on the nanotubes is below this pressure, whereas the other one is above it. When the temperature increases, this distinguishable stepwise adsorption behavior is less pronounced, and above 103 K the substeps disappear, as can be seen in Figures 2 and 3.

Adsorption Sites and Energy of Adsorption from ab Initio and Molecular Mechanical Calculations. Geometry optimizations (Figure 4) resulting from MM+ and DFT methods show that, on the external surface (S) (Figure 5, top left) as well as on the inner sites (T) (Figure 5, bottom left), the methane molecules place themselves so that three of the H atoms point to the closest tube surface. For Groove sites (G), the methane molecules are ordered with two of its H atoms lying along the curved channel formed by the two corresponding nanotube surfaces, parallel to the nanotube's axis (see Figure 5, top right). Inside the interstitial channel (IC), three H atoms of the methane molecules point to the three gaps (Figure 5, bottom right). Energies obtained from both methods employed are presented in Tables 2 and 3, and plotted in Figures 9a, 10a, and 11a. The corresponding experimental values are given in Table 4.

We can see for external of G and S sites that they are better represented by (7,7) and (12,12) nanotubes and that the interaction energy corresponding to G sites is approximately twice that of S sites, in good agreement with experiments and first principles calculations.[8,34,36,37] For internal T and IC sites, the

(30) Albesa, A. G.; Vicente, J. L. *J. Arg. Chem. Soc.* **2007**, *95*, 48.
(31) Li, A. H. T.; Chao, S. D. *J. Chem. Phys.* **2006**, *125*, 94312.
(32) Tzuzuki, S.; Luthi, H. P. *J. Chem. Phys.* **2001**, *114*, 3949.
(33) Martin, M.; Siepmann, J. I. *J. Phys. Chem. B* **1998**, *102*, 2569.
(34) Albesa, A. G.; Filippin, A.; Vicente, J. L. *Inf. Tecnol.* **2009**, *20*, 31.
(35) Talapatra, S.; Zambano, A. Z.; Weber, S. E.; Migone, A. D. *Phys. Rev. Lett.* **2000**, *85*, 138.
(36) Calbi, M. M.; Gatica, S. M.; Borjan, M. J.; Cole, M. W. *J. Chem. Phys.* **2001**, *115*, 9975.
(37) Ricca, A.; Bauschlicher, C. W. *Chem. Phys.* **2006**, *324*, 455.

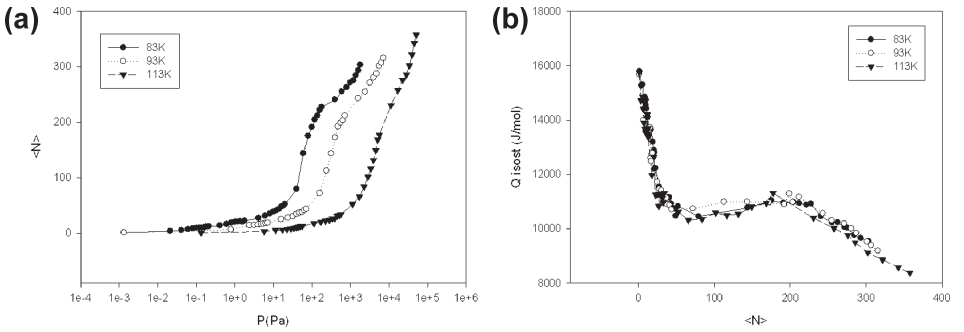

Figure 6. (a) Simulated isotherm at 83, 93, and 113 K for closed end tubes of diameter 9.49 A (7,7) SWNT; (b) corresponding isosteric heat of adsorption.

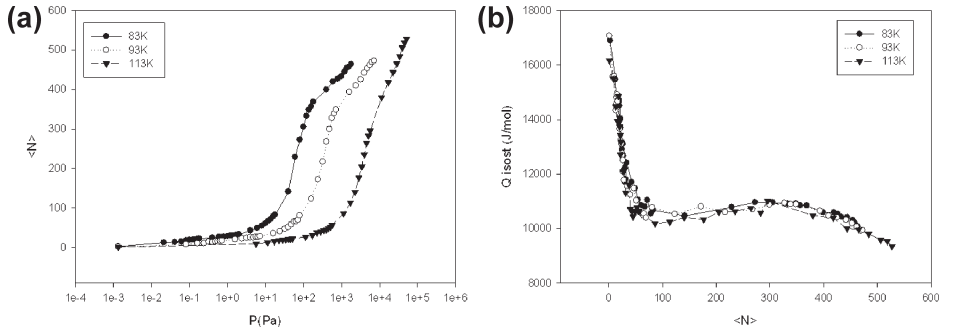

Figure 7. (a) Simulated isotherm at 83, 93, and 113 K for closed end tubes of diameter 16.28 A (12,12) SWNT; (b) corresponding isosteric heat of adsorption.

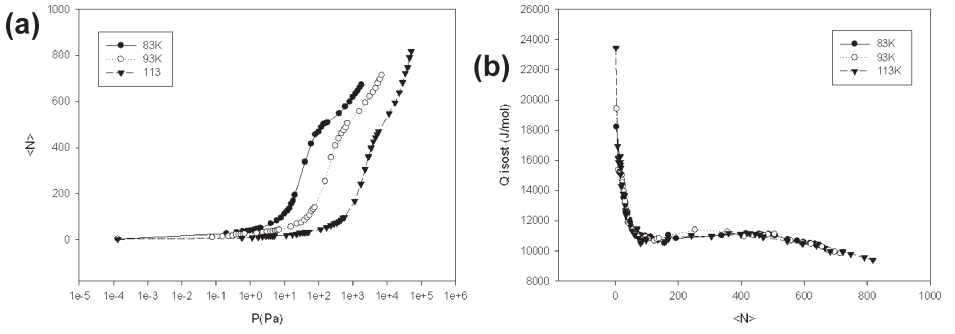

Figure 8. (a) Simulated isotherm at 83, 93, and 113 K for closed end tubes of diameter 20.34 A (15,15) SWNT; (b) corresponding isosteric heat of adsorption.

agreement between MM+ and DFT calculations is somehow poorer, probably due to the different cluster employed. In spite of these differences, both results showed the same trends when the tube diameter is increased.

We can summarize the comparison of the behavior of the binding energies for these four sites as a function of nanotube diameter as follows: the binding energy of site S is almost constant and weaker than the other sites, in the case of site G it slightly decreases as the diameter increases, a behavior that is opposite to that of the ICs, and, finally, the binding energy of site T clearly decreases as the nanotube diameter increases.

Nevertheless, for the (15,15) nanotubes the MM+ and the DFT calculations show that the IC sites are the most favorable sites for adsorption, in contrast with the conclusions derived from the experimental data.[35] Since in all likelihood the diameters of the nanotubes used in the experiments were smaller than those of the (15,15) nanotubes used in the calculations, this difference does not constitute a contradiction between the two sets of results. One considers the IC sites for the (15,15) bundle, because they can mimic defect-induced IC sites of an heterogeneous bundle. We see from Tables 2 and 3, relatively high interaction energies for IC sites of (15,15) bundle (−36.1 and −18.5 KJ obtained using MM+ and DFT calculations, respectively); these results confirm the adsorption sites as preferred in low pressures regime. However, when comparing the above-mentioned values with the corresponding for G sites of (7,7) and (12,12) bundles, we observed the opposite tendency (i.e., MM+ gives lower values, but DFT gives higher values).

Isotherms, Adsorption Sites and Isosteric Heat of Adsorption from Monte Carlo Simulations. *SWNTs Closed at Both Ends*. Isotherms and isosteric heat of adsorption, determined from the computer simulations, for capped SWNTs are shown in Figures 6−8 for the three different diameters explored. There are no significant differences between the isotherms, in terms of their behavior as a function of relative coverage. The main difference between the isosteric heat of adsorption values for (15,15) SWNTs and the other two sets of nanotubes is that these tubes, in spite of the fact that they are

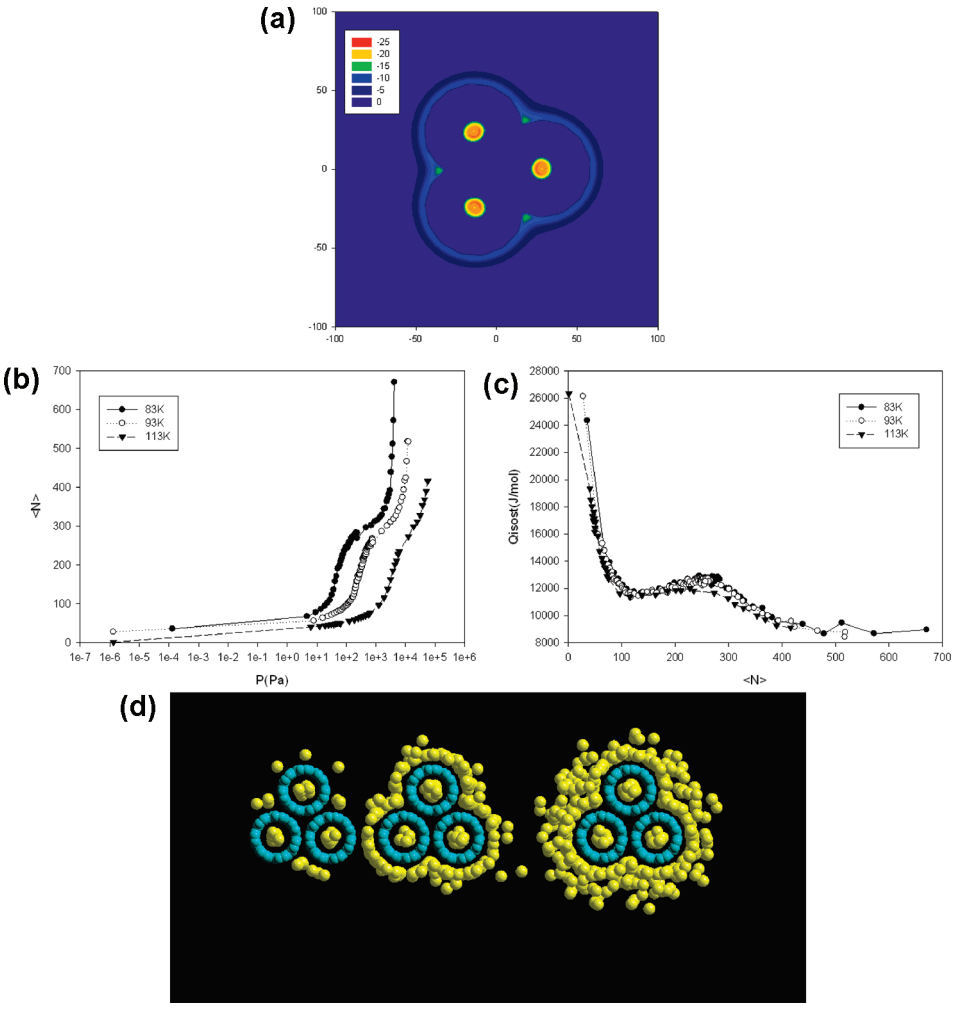

Figure 9. (a) Minimum of binding energy profiles along the tube (If $E \geq 0$, then we set $E = 0$), for opened end tubes of diameter 9.49 A (7,7) SWNT; in kJ/mol and arbitrary axes units; (b) corresponding isotherm at 83, 93, and 113 K; (c) isosteric heat of adsorption; (d) upper view of filling evolution corresponding to isotherm at 113 K and pressures of 0.062, 5.0, and 56.3 KPa.

closed, have a high energy site in the interstitial channels (IC sites). For the (15,15) nanotubes the ICs are the sites with the highest binding energy, followed by the grooves (G) and the surface sites (S).

In the (7,7) and (12,12) structures, the groove sites (G) are the highest binding energy sites followed by the external surfaces of the bundles. Adsorption on the ICs is unfavorable energetically. As a result of this similarity in behavior the energetic profiles are similar when the coverages are normalized by the monolayer capacity.

In Figures 9d, 10d, and 11d,f, without considering T sites, we identify the contribution of different adsorption sites for the isotherm simulated at 113 K for (7,7) and (12,12) structures, respectively. For groove sites, G, of (7,7) nanotubes, we note that first and second layers are completed approximately at 0.05, and 1.0 KPa, while for the surface sites the completions occur at 3.5 and 45.0 KPa. For (12,12) nanotube groove layers become completed approximately at 0.01, and 0.45 KPa, and for surface layers the corresponding pressures are 3.5, and 45.0 KPa. If we compare the difference between the chemical potentials of (7,7) and (12,12) SWNTs for the first layer of groove site with the interaction energy resulting from ab initio and molecular mechanical calculations, we find 1.5 KJ, in good agreement with that given in Tables 2 and 3. But for the first layer of surface sites, there is no difference between the chemical potential of (7,7) and (12,12) nanotubes. We think that this happens because the calculations were performed for only one CH_4 molecule which can be certainly true for the first adsorption on groove sites (when one can assume that no other molecules are adsorbed nearby), but not for adsorption on other surface sites, because in this case there are other molecules adsorbed on surrounding sites. The same argument can be applied to other layers. On the other hand, we found that the pressure required to complete the first groove layer for (7,7) and (12,12) nanotubes is similar to the corresponding value to fill the interstitial channel of (15,15) bundle.

Our simulation results show that whether or not the IC sites are occupied by methane molecules depends on the nanotube diameter. If the diameter is lower than 16 A, methane does not adsorb on the interstitial channels,[38] but over this limit the IC sites become favorable to adsorption.

SWNTs Opened at Both Ends. Isotherms for an arrangement of three open-ended (7,7) nanotubes, simulated at three different temperatures, are shown in Figure 9b. We can see that at very low pressures, the nanotube's inner sites are completely filled. These sites have the highest energy binding sites in the bundles as a result of the small diameter of the tubes and the close proximity between the C atoms in the walls of the nanotubes and the methane

(38) Teizer, W.; Hallock, R. B.; Dujardin, E.; Ebbesen, T. W. *Phys. Rev. Lett.* **1999**, *82*, 5305.

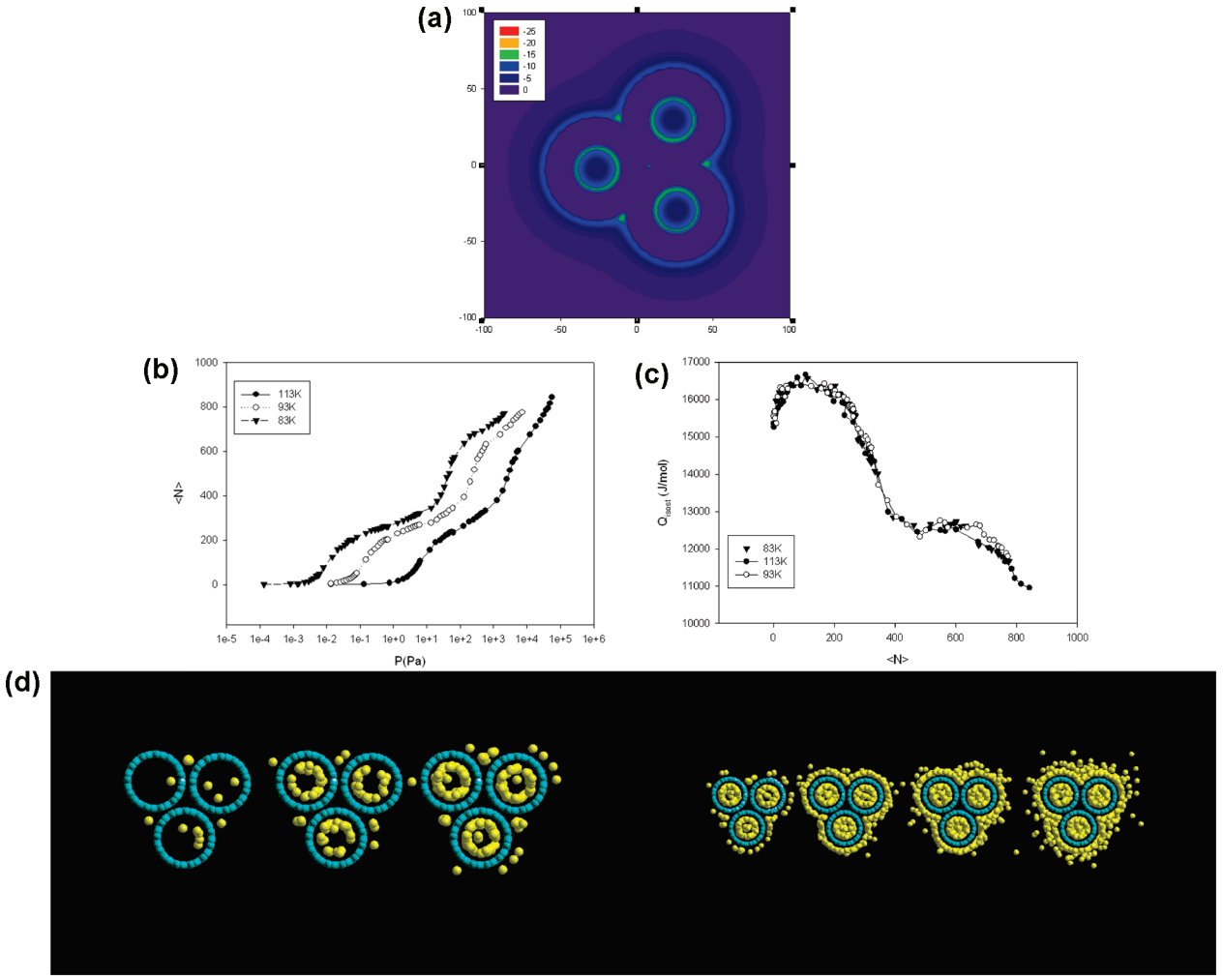

Figure 10. (a) Minimum of binding energy profiles along the tube (if $E \geq 0$, then we set $E = 0$), for opened end tubes of diameter 16.28 A (12,12) SWNT; in kJ/mol and arbitrary axes units; (b) corresponding isotherm at 83, 93, and 113 K; (c) isosteric heat of adsorption; upper view of filling evolution corresponding to isotherm at 113 K and pressures of (d) 0.00138, 0.00627, 0.0563 KPa; 0.563, 5.63, 25.0, and 56.3 KPa.

molecules. This effect can be more clearly seen in the potential energy curves (Figure 9a) and in the isosteric heat of adsorption plot (Figure 9c). The next highest binding energy sites for the (7,7) nanotubes are the grooves, followed by the outside surface of the NT (Figure 9d). As is the case with all surfaces with a high degree of graphitization, the isosteric heat of adsorption shows a peak characteristic of the completion of the first monolayer. It is interesting to note that adsorption in the second layer starts in the second layer groove sites.[36,40]

In the (12,12) nanotubes, at low pressures, methane molecules adsorb inside the nanotubes and on the groove sites (Figure 10d). As the pressure grows, a monolayer starts forming on the inside surface of the nanotubes. This appears in the simulated isotherms as a "knee" at low pressures and as a peak in isosteric heat of adsorption value at low coverage. After the interior layer is completed, a new high energy site appears in the axial phase,[39] inside the nanotubes. When these centers are filled, adsorption continues on the surface. As in the case of (7,7) nanotubes, the second layer begins on the groove sites.

The minimum in binding enrgy profiles (Figure 10a) shows that ICs are a possible adsorption site, but this minimum is only founded at the end of the simulation box (end of the tubes), and they do no represent real IC sites because the other values along IC position are repulsive, then we do not observe any methane molecules in the (12,12) interstitial channels.

In the energy diagram for the (15,15) nanotubes, we see (Figure 11) that IC sites are the ones with the highest adsorption energy. At very low pressures, these sites are occupied by methane molecules. This is also shown in the isosteric heat of adsorption curve. The next two highest values of the binding energy are those for the interior sites and the grooves (the order in which the energies for these two groups of sites follow the ICs is different in the DFT calculations and in the MM+ ones). After the first layer inside the nanotubes is completed, adsorption continues on the external surface, but not in the central zone inside the nanotubes, as was the case for the (12,12) nanotubes. When the external layer is completed, we observe a peak in the isosteric heat of adsorption.

In all nanotubes we can see that the pressure required to fill inner (T) sites is lower than that for the completion the second layer groove (G) sites and the first layer of the surface (S) sites, but is greater than that needed to occupied the IC sites, the latter in the case of (15,15) bundles.

If we compare the simulated isotherms from closed homogeneous bundles with experimental data from HiPco SWNTs, we find a very good fit in the range of high pressures, where the major contribution to adsorption is made by surface (S) sites, while at lower pressures (i.e., in the intermediate coverage region), we

(39) Tasca, R. A.; Calbi, M. M.; Cole, M. W. *Phys. Rev. E* **2002**, *65*, 061607.
(40) Talapatra, S.; Krungleviciute, V.; Migone, A. D. *Phys. Rev. Lett.* **2002**, *89*, 246106.

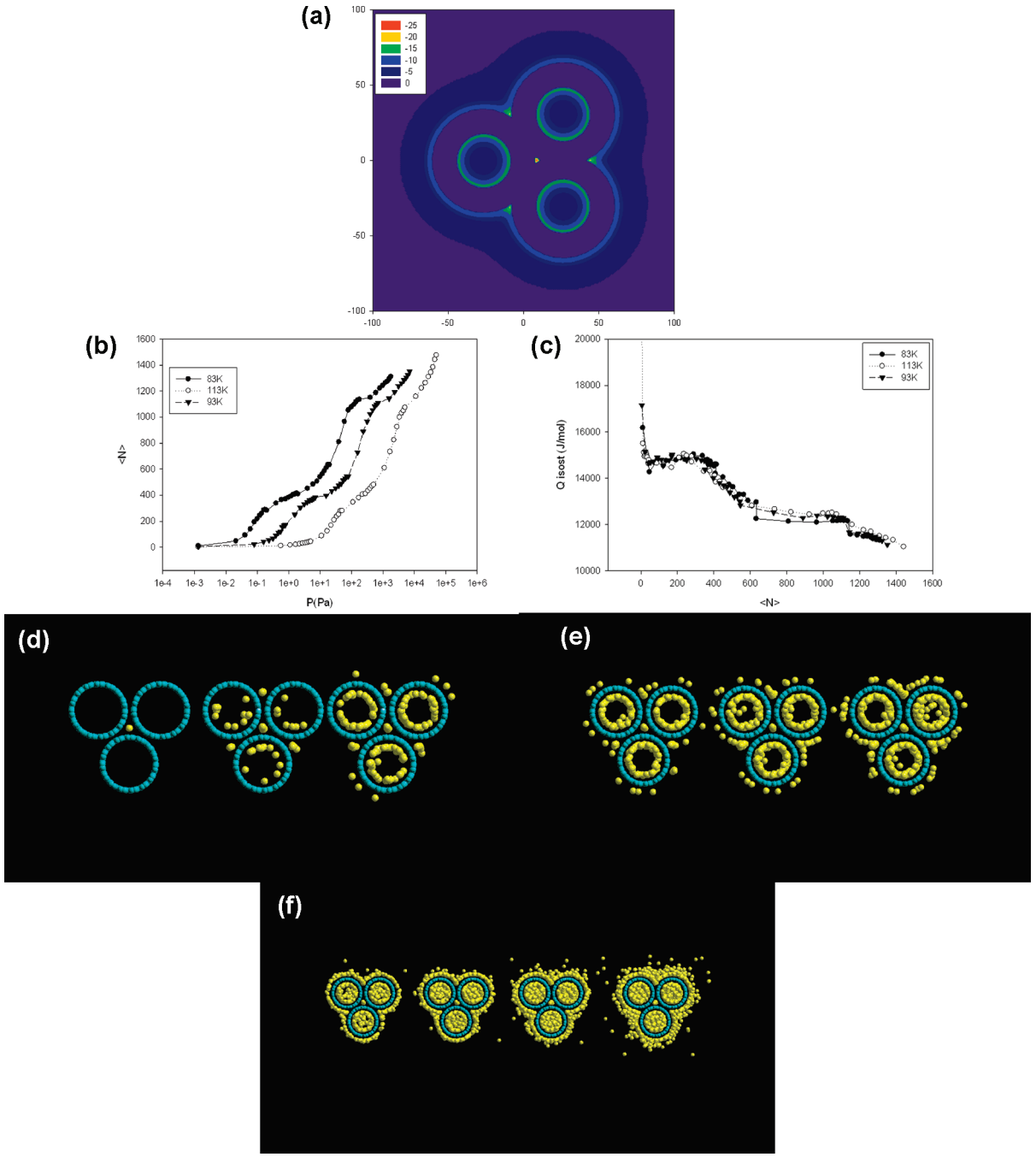

Figure 11. (a) Minimum of binding energy profiles along the tube (if $E \geq 0$, then we set $E = 0$), for opened end tubes of diameter 20.34 A (15,15) SWNT; in kJ/mol and arbitrary axes units; (b) corresponding isotherm at 83, 93, and 113 K; (c) isosteric heat of adsorption; upper view of filling evolution corresponding to isotherm at 113 K and pressures of (d) 0.0000133, 0.00509, 0.0226 KPa; (e) 0.0509, 0.226, 0.509 KPa; (f) 2.26, 5.09, 22.6, and 45.2 KPa.

Table 4. Interaction Energies from Experimental Values[5]

experimental values [KJ]	S	G
ref 34.	−11.21	−18.28
ref 8.	−10.46	−24.27

observe qualitative differences (see Figure 12). These differences cannot be attributed to interstitial channel (IC) sites (case (15,15) bundles in Figure 11), because these sites participate at very low pressures. On the other hand, open homogeneous bundles fit better the experimental data in this intermediate coverage region because the contribution inside the tubes (T) continues in this region. These results not only confirm the quality of the atomistic models[6] used to describe the adsorbed phase over the whole range of pressures, as a result of better substrate representation, but also show that a complete description of adsorption on HiPco SWNTs, that takes into account what happen beyond very low pressures, has to consider the contribution of open tubes in the bundles, regardless of how significant are the IC sites.

Comparison between CH_4 Adsorption on SWNT and on Graphite Surfaces. As was noted before, the values of the experimentally measured pressures for the two substeps in the first layer of methane on carbon nanotubes fall on either side of the value of the pressure corresponding to the single step present

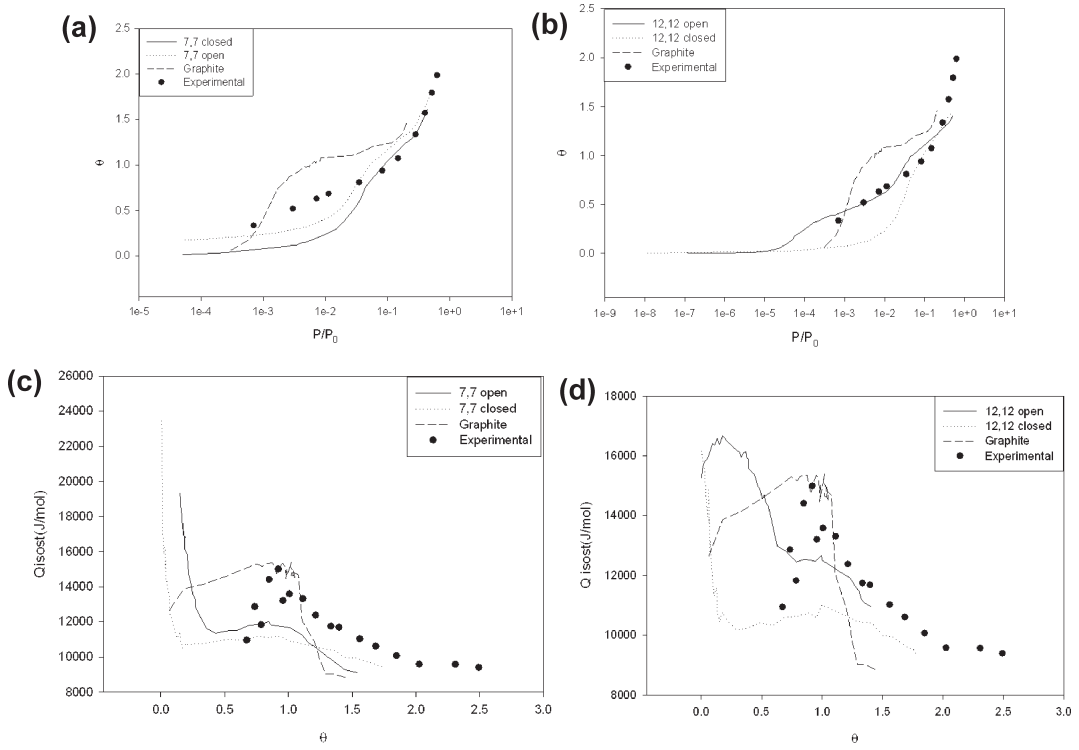

Figure 12. (a) Isotherms at 113 K. Experimental results from SWNT (circles), are compared with simulations of (7,7) bundles with closed (solid line) and opened end (dotted line), and also with experimental results of CH_4 adsorbed on graphite (dashed line). $P_0 = 114.469$ KPa is the saturation pressure at 113 K; (b) same isotherms as in panel a but using (12,12) bundles in the simulations; (c) experimental and simulated isosteric heat of adsorption with the same bundles and notation as in panel a; (d) experimental and simulated isosteric heat of adsorption with the same bundles and notation as in panel b.

for the adsorption of methane on planar graphite. Hence, the higher binding energy sites on the nanotubes have a value of the binding energy that is larger than that for methane on graphite, and the lower binding energy sites on the nanotubes have a value that is smaller than that.

In Figure 12a and 12b we compared the 113 K isotherms, with values calculated for nanotubes of closed and opened ends, and also for graphite, for two kinds of the studied nanotubes, that is, (a) for (7,7) bundle and (b) (12,12) bundle. Experimental values are higher than those calculated for closed end nanotubes and lower than those for graphite (except at very low pressures). On the other hand, for opened nanotubes, the calculated values correspond to a lesser amount of adsorbed molecules in the low pressures regime and to a greater amount in the high pressure regime. If we compare in Figure 12b, above 10^{-5} relative pressures (that correspond approximately to 10^{-3} KPa), simulations of opened and closed nanotubes, we note that the first fits experimental results much better the second and confirms, from Figures 10d and 11d that a complete description of adsorption on this type of SWNTs (HiPco) has to consider the contribution of open tubes in the bundles independently of the role played by the adsorption on large IC sites.

When comparing the pressure needed for monolayer completion, we observed a lower value for graphite than nanotubes; a possible explanation can be found analyzing the isosteric heat of adsorption. In Figure 12c and 12d we compare the isosteric heats of adsorption obtained at 113 K, derived from eq 1, with the values calculated for closed and opened-end nanotubes, and also for graphite, for the two kinds of studied nanotubes, that is, 12c for (7,7) bundle, and 12d for (12,12) bundle.

We note that the isosteric heat of adsorption is higher for graphite than for the nanotubes for all cases, except for the lowest coverages (where the isosteric heat is higher for the nanotubes). The higher values for the energy on graphite for the first layer, can be attributed to different contributions of gas−solid and gas−gas interactions. The stronger gas−solid interactions are due to the fact that the nanotubes are single-walled, while graphite is formed by many graphene layers. The curvature also has a significant effect; and it makes the gas−gas interaction in the nanotubes weaker than on graphite. When the monolayer is formed, the number of neighboring molecules on graphite corresponds to the 2D case, but on the curved nanotube surface, each methane molecule is surrounded by a smaller number of neighbors. In the case of open-ended nanotubes, there are additional differences in the low coverage region, owing to the presence of the inner sites (T). We note that the curvature at the interior of the nanotube favors interactions between neighboring adsorbate molecules, and we can see, as a result, an increase in the contribution of the gas−gas interactions to the isosteric heat of adsorption.

Experimental values of the isosteric heat of adsorption, in Figure 12c,d, show that closed-ended nanotubes describe well the behavior only in the high-coverage region. To explore the intermediate coverage region, contribution of opened-ended nanotubes must be taken into account (see Figure 12b). Nevertheless, near the monolayer completion ($\theta = 1$), q_{st} values are greater than those predicted by opened SWNTs, and taking into account that the increase is of the order of the one obtained for graphite, the difference can be attributed to other carbonaceous forms present in the sample. These impurities overlap the effect of open and close SWNTs and limit the possibility of estimating the fraction of open-ended tubes in the bundles; that is, in the high-pressures regime, closed and open-ended nanotubes isotherms resemble each other, but near the monolayer completion the presence of unknown quantities of other carbonaceous forms hinder and

render difficult the determination of the percentage of open-ended tubes in the bundle. Moreover, there are more than two types of tubes because the percentage of impurities must be taken into account.

Conclusions

We have conducted experimental adsorption isotherms and isosteric heat determinations for methane adsorbed on close-ended single-walled carbon nanotubes of HiPco SWNTs. Our results are in good agreement with those previously reported for this system. We interpret our adsorption results by attributing the high binding energy adsorption to the grooves or G sites, to the few large diameter defect-induced interstitials present on the bundles, and to the low binding energy adsorption to surface or S sites as well as the contribution of a percentage of open tubes in the bundles.

We carried out ab initio and molecular mechanical calculations in order to compute the binding energies of all possible adsorption sites in homogeneous bundles of nanotubes. We found that for nanotubes with smaller diameters, methane's binding energy is greater on G sites than on S sites. When the diameter is large enough (at least greater than 20 A) the highest binding energy corresponds to the ICs sites, followed by G sites and finally the S sites. In the case of opened tubes the T sites have the greatest binding energy.

All possible scenarios attempting to give a complete description of the adsorption processes on single-walled carbon nanotubes are strongly dependent on the nanotube diameters. This dependence suggests that perhaps it would be useful to classify the bundles according to the diameter of the tubes involved in a manner analogous to that used for pore size classification for other porous substrates.

For closed tubes, the complete scenario would be as follows: adsorption starts as linear chains (1D process) at the strongest binding energy sites. These strongest sites are the G sites in case of narrow tubes, but beyond a critical value of tube diameter (which would be different for different molecules, depending on their diameter), the IC sites become more relevant. After these sites are filled, adsorption proceeds on the external surface of the bundles (2D process).

In the case of open tubes the scenario is more complex. While for very narrow tubes it can be assumed for a simple 1D process inside narrow nanotubes, that when the diameter of the tubes becomes larger, the inner tube sites fill like the internal surface of a cylindrical pore after the IC sites are completely occupied. Depending on the diameter of the tubes, the values of the binding energies on the interior surfaces are comparable to those for the grooves. The outer surface sites S always have the lowest binding energy.

Comparing simulated isotherms with the adsorption on graphite we note that the monolayer on graphite is completed at a pressure below that corresponding to the nanotubes, and that the isosteric heat of adsorption is greater for graphite. This is due to the greater gas−solid interaction for the graphite case, because the nanotubes are single-walled, while graphite is formed by several graphene layers. The gas−gas interaction on the nanotubes is weaker than on graphite, because the curvature of the nanotubes reduces the number of neighboring adsorbate molecules in this case, relative to those present in the graphite case.

The results confirm the quality of the atomistic models[6] used to analyze the adsorbed phases over the whole range of pressures, as a result of better substrate representation, and show that a complete description of adsorption on HiPco SWNT, that takes into account intermediate pressures, has to consider the presence of carbonaceous impurities and the contribution of open tubes in the bundles, regardless of how significant is the role played by the IC sites at very low pressures.

Acknowledgment. This work was completed with the support of the Universidad Nacional de La Plata (UNLP), the Comisión de Investigaciones Científicas de la Provincia de Buenos Aires (CICPBA), and the Consejo de Investigaciones Científicas y Tecnológicas (CONICET).